



Published in final edited form as:

Nat Neurosci. 2020 September ; 23(9): 1047–1050. doi:10.1038/s41593-019-0473-5.

Revaluation of magnetic properties of Magneto

Guangfu Wang^{1,2}, Peng Zhang^{1,2}, Suresh K. Mendu^{1,2}, Yali Wang¹, Yajun Zhang¹, Xi Kang¹, Bimal N. Desai^{1,3}, J. Julius Zhu^{1,3}

¹Department of Pharmacology, University of Virginia School of Medicine, Charlottesville, VA 22908, USA

²These authors contributed equally to this work

³Correspondence and requests for materials should be addressed to Bimal Desai and Julius Zhu

Magnetic control of neuronal activity offers many obvious advantages over electric, optogenetic and chemogenetic manipulations. A recent paper claimed the development of a magnetic actuator, Magneto, that is effective in controlling neuronal firing¹, although its mechanism of action is difficult to reconcile in light of certain physics principles². We found that neurons expressing Magneto did not respond to magnetic stimuli with any membrane depolarization (let alone action potential), although these neurons frequently generated spontaneous action potentials. Because the previous study did not establish the precise temporal correlation between magnetic stimuli and action potentials in recorded neurons¹, the reported magnetically-evoked action potentials are likely to represent mismatched spontaneous firings.

To examine the membrane surface incorporation of Magneto, we transfected 293T cells with the P2A-linked wild type TRPV4 (the primogenitor of Magneto2.0), ferritin (the other key element of Magneto2.0) and mCherry, aka TRPV4-P2A-ferritin-P2A-mCherry, or P2A-linked Magneto2.0 and mCherry, aka Magneto-P2A-mCherry. We then made simultaneous measurements of the magnetic stimulation- and agonist-evoked responses in control non-expressing and TRPV4-P2A-ferritin-P2A-mCherry or Magneto-P2A-mCherry expressing cell pairs (Fig 1a). To determine the precise timing of applied magnetic field, we used an LED illuminator and a photodetector to monitor the exact position of magnets mounted on a Luigs-Neumann manipulator. Delivering a K&J N42 neodymium 1/16" block magnet to the position 1,000 μm away from recorded cells generated a 64.5-mT magnetic field (Fig S1). As expected, delivery and withdrawal of the magnet did not induce any current in control and TRPV4-P2A-ferritin-P2A-mCherry expressing cells (Fig 1b-c). In contrast, puff application of TRPV4 agonist, GSK1016790A (**GSK101**), reliably elicited inward currents in TRPV4-P2A-ferritin-P2A-mCherry expressing cells, but not control non-expressing cells

Address for correspondence: J. Julius Zhu, Department of Pharmacology, University of Virginia School of Medicine, 1300 Jefferson Park Avenue, Charlottesville, VA 22908, Tel: (434) 243-9246, Fax: (434) 982-3878, jjzhu@virginia.edu.

AUTHOR CONTRIBUTIONS

G.W., P.Z. and S.K.M. carried out the experiments with assistance from Y.W., Y.Z. and X.K.; B.N.D. and J.J.Z. wrote the manuscript with input from all coauthors.

DECLARATION OF INTERESTS

The authors declare no competing interests.

(Fig 1b-c). The GSK101-elicited currents in TRPV4-P2A-ferritin-P2A-mCherry expressing cells had the IV relationship typical of TRPV4, and were blocked by a TRPV4 antagonist GSK205 (Fig S2a-b), indicating TRPV4-specific currents³. Surprisingly, neither the magnetic stimuli nor GSK101 induced any significant current in control and Magneto-P2A-mCherry expressing cells (Fig 1b-c). Together, these results suggest that unlike wild type TRPV4, Magneto2.0 fails to form a functional ion channel and/or incorporate into the plasma membrane of 293T cells.

Next, we expressed mCherry-fused Magneto2.0, aka Magneto-Ts-mCherry, and Magneto-P2A-mCherry in CA1 neurons of cultured rat hippocampal slices using the established Sindbis viral expression system^{4,5} (Fig 1d). Two-photon images showed that Magneto-Ts-mCherry, although robustly expressed, seemed to have limited, if any, presence at the plasma membrane of CA1 neurons (Fig 1d **insets**). Consistently, Western blots showed that in contrast to TRPV4 in TRPV4-P2A-ferritin-P2A-mCherry expressing CA1 cells, Magneto2.0 membrane surface expression was minimal despite its high intracellular expression in Magneto-P2A-mCherry expressing CA1 cells (Figs 1e-g **and** S9). Expression of Magneto-P2A-mCherry and TRPV4-P2A-ferritin-P2A-mCherry in the mouse barrel cortex *in vivo* for 7-10-days, using the established lentiviral expression system⁴, verified only TRPV4, but not Magneto2.0, had efficient membrane surface expression in cortical neurons despite high intracellular expressions (Fig S3 **and** S10). These results are consistent with the deletion of C-terminus of TRPV4, essential for its surface trafficking/functional expression³, in Magneto2.0¹. Subsequent simultaneous whole-cell recordings showed that application of up to 64.5 mT static magnetic field induced neither depolarization nor action potential firing in control and Magneto-P2A-mCherry expressing CA1 cells (Fig 1h-i). Similarly, the magnetic stimuli failed to induce depolarization and action potential in CA1 cells lentivirally expressing Magneto-P2A-mCherry (Fig S4). These results indicate that the magnetic stimuli do not induce action potential in Magneto expressing CA1 neurons in cultured slices.

We further made *in vivo* Sindbis viral expression of Magneto-P2A-mCherry in layer 2/3 (**L2/3**) pyramidal and stellate neurons in the mouse medial entorhinal cortex (**MEC**) or L5 pyramidal neurons in the mouse barrel cortex for ~18 hrs, and then acutely prepared entorhinal or barrel cortical slices (Figs S5a **and** S6a). Simultaneous recordings showed that the 64.5 mT static magnetic field did not induce any depolarization or action potential in control and Magneto-P2A-mCherry expressing neurons (Figs S5-6). Moreover, positioning the same 3/8" permanent block magnet employed in the previous study¹ at 5.00 mm away from recorded neurons, which yielded a 78.8 mT static magnetic field (Fig S1), induced neither depolarization nor action potential in control and Magneto-P2A-mCherry expressing entorhinal neurons (Fig S7a-c). We noted that control and Magneto-P2A-mCherry expressing entorhinal neurons frequently displayed spontaneous synaptic events, and at times, the spontaneous events reached the threshold and triggered bursts of action potentials (Figs S5b, S5d **and** S7b), suggest a potential cause for the reported magnetic effects¹.

We then recorded hippocampal neurons after ~3-5-week *in vivo* AAV viral expression of DIO-Magneto and GFP-Cre (Fig S8a), using the same brain slice tissues prepared and published in *Wheeler et al.*¹. The 78.8 mT static magnetic field induced neither depolarization nor action potential discharge in control or Magneto expressing dentate gyrus

neurons (Fig S8b-c). Finally, we made *in vivo* AAV viral expression of DIO-Magneto and GFP-Cre in L2/3 of mouse MEC for ~3-5 weeks, and then recorded activity of entorhinal neurons in acutely prepared entorhinal cortical slices (Fig 1j). Again, application of up to 64.5 mT static magnetic field did not induce any depolarization or action potential firing in control and DIO-Magneto/GFP-Cre expressing entorhinal neurons (Fig 1k-l). Importantly, we observed abundant spontaneous activities that from time to time, reached the firing threshold and elicited action potentials in these experiments (Figs 1k-m). Collectively, our results consistently support the idea that Magneto does not function as an effective magnetic actuator and spontaneous action potentials can confound the interpretation of Magneto expressing neurons subjected to magnetic stimuli.

In summary, we systematically interrogated Magneto2.0 with multiple approaches (i.e., transfection, Sindibis, lentivirus, and AAV viral expression *in vitro* and/or *in vivo*), multiple cell types (i.e., 293 cells, hippocampal CA1, dentate gyrus, cortical L5 pyramidal, entorhinal L2/3 stellate and pyramidal neurons), and multiple animal species (i.e., rats and mice). Our results, together with two accompanied studies that used additional approaches (e.g. FSV viral expression), cell types (e.g., cerebral Purkinje and barrel cortical L2/3 neurons), and manipulation/recording methods (e.g., electric magnetic stimuli and *in vivo* recordings)^{6,7}, consistently demonstrate that Magneto2.0 did not respond to magnetic stimuli with any membrane depolarization (let alone action potential). These results also raise the concern about two other recently reported magnetic actuators, MagR and α GFP-TRPV1/GFP-ferritin, considering that the temporal correlation between magnetic stimuli and neuronal activity established in neither of the reports^{8,9} and our futile attempts to reproduce their electrophysiology findings (G.W., P.Z, and J.J.Z. unpublished data). These underscore the importance of (re)establish a set of rigorous criteria to aid continuing tool-engineering efforts, including building of a magnetogenetic toolbox. As exemplified in our comprehensive testing of Magneto, the criteria may include: first, surface expression validation; second, functional validation; and third, electrophysiological validation. Obviously, going beyond the proof-of-principle to address unresolved fundamental biology question(s), which is typically included in previous patch-clamp and imaging technology development studies, yet frequently missing in recent methodology papers, will further ensure the applicability of tools developed.

METHODS

Animal preparation

Male and female Sprague Dawley rats and C57BL/6 mice were used to prepare cultured slices and acute slices used in this study. Animals were maintained in the animal facility at the University of Virginia, and family or pair housed in the temperature-controlled animal room with 12-h/12-h light/dark cycle. Food and water were available *ad libitum*. All procedures for animal surgery and maintenance were performed following protocols approved by the Animal Care & Use Committee of the University of Virginia and in accordance with US National Institutes of Health guidelines.

Cultured slice preparation

Cultured slices were prepared from postnatal 6–7 day old rats or mice (P6–7) as reported in our previous studies^{4,5}. In brief, the hippocampi were dissected out in ice-cold HEPES-buffered Hanks' solution (pH 7.35) under sterile conditions, sectioned into 400- μ m slices on a tissue chopper, and explanted onto a Millicell-CM membrane (0.4- μ m pore size; Millipore). The membranes were then placed in 750 μ l of MEM culture medium, contained (in mM): HEPES 30, heat-inactivated horse serum 20%, glutamine 1.4, D-glucose 16.25, NaHCO₃ 5, CaCl₂ 1, MgSO₄ 2, insulin 1 mg/ml, ascorbic acid 0.012% at pH 7.28 and osmolarity 320. Cultured slices were maintained at 35°C, in a humidified incubator (ambient air enriched with 5% CO₂).

Constructs of recombinant proteins and expression

All constructs, including TRPV4-P2A-ferritin-P2A-mCherry, Magneto-P2A-mCherry and Magneto-Ts-mCherry were generously supplied by Drs Chris Deppmann and Ali Güler. Magneto-P2A-mCherry and Magneto-Ts-mCherry were subcloned into Sindbis and lentiviral vectors. AAV viral solutions of the Cre-dependent Magneto2.0 AAV virus, aka AAV1-CMV::DIO-Magneto, and AAV9-Camk2a::EGFP-Cre were also supplied by Drs Chris Deppmann and Ali Güler. For expression in cultured 293T cells, Magneto-P2A-mCherry and TRPV4-P2A-ferritin-P2A-mCherry were transfected using the calcium phosphate transfection method. For expression in cultured slices, CA1 pyramidal neurons in hippocampal cultured slices were infected after 8–18 days *in vitro* with lentivirus or Sindbis virus, and then incubated on culture media and 5% CO₂ before experiments. For expression in intact brains, P18–28 mice were initially anesthetized by an intraperitoneal injection of ketamine and xylazine (10 and 2 mg/kg, respectively). Animals were then placed in a stereotaxic frame and one or multiple small (~1×1 mm) holes were opened above the cortex. A glass pipette was used to make pressure injections of ~100 nl Sindbis or lentiviral solution, or 200 nl equivolume mixture of AAV viral solutions of AAV1-CMV::DIO-Magneto and AAV9-Camk2a::EGFP-Cre into the barrel cortex, hippocampus and/or MEC according to their stereotaxic coordinates. After injection, animals were allowed to recover from the anesthesia and returned to their cages. Experiments were typically performed within 18±2 hours after Sindbis viral infection, 7–10 days after lentiviral infection and 3–5 weeks after AAV viral infection.

Biochemical analysis

Hippocampal extracts were prepared by homogenizing hippocampal CA1 regions isolated from cultured slices, while cortical extracts were prepared by homogenizing mCherry expressing barrel cortical areas isolated from acute cortical slices. Membranes were blotted with anti-FLAG antibody (1:5,000 for *in vitro* expression, 1:2,000 for *in vivo* expression; Fisher Scientific, Hampton, NH; Cat# MA1-91878, RRID:AB_1957945), stripped and reblotted twice with anti-GluA1 (1:1,000 for *in vitro* expression; 1:1,000 for *in vivo* expression; EMD Millipore, Burlington, MA; Cat# AB1504, RRID:AB_2113602) or anti-GluA2 antibody (1:6,000 for *in vitro* expression; 1:6,000 for *in vivo* expression; EMD Millipore; Cat# AB1768, RRID:AB_2313802). Western blots were quantified by

chemiluminescence and densitometric scanning of the films under linear exposure conditions.

Electrophysiology and two-photon imaging

Simultaneous multiple whole-cell recordings were obtained from nearby expressing and non-expressing 293T cells, CA1 pyramidal neurons, barrel cortical layer 5 (L5) pyramidal neurons, dentate gyrus neurons, entorhinal L2/3 stellate and pyramidal neurons, under visual guidance with fluorescence and transmitted light illumination^{5,10}, using up to two Axopatch-200B (voltage clamp) or Axoclamp 2B (current clamp) amplifiers (Molecular Devices, LLC, Sunnyvale, CA). Bath solution (29±1.5°C), unless otherwise stated, contained (in mM): NaCl 119, KCl 2.5, CaCl₂ 2, MgCl₂ 1, NaHCO₃ 26, NaH₂PO₄ 1, glucose 25, at pH 7.4 and gassed with 5% CO₂/95% O₂. Patch recording pipettes (3–6 MΩ) for current (voltage-clamp) recordings contained (in mM): cesium methanesulfonate 115, CsCl 20, HEPES 10, MgCl₂ 2.5, Na₂ATP 4, Na₃GTP 0.4, sodium phosphocreatine 10, EGTA 0.6, and spermine 0.1, at pH 7.25; and for voltage (current-clamp) recordings contained: potassium gluconate 115, HEPES 10, MgCl₂ 2, MgATP 2, Na₂ATP 2, Na₃GTP 0.3 and KCl 20, at pH 7.25.

Two-photon imaging and electrophysiology were simultaneously performed using a custom-built microscope operated by a custom-written IGOR Pro 6 program (WaveMetrics, Lake Oswego, OR), PEPOI^{4,10}, which is available at the University of Virginia Patent Foundation (contact <https://ivg.virginia.edu/> for the end user license). Neighboring expressing and non-expressing CA1 or dentate gyrus neuron pairs were broken in simultaneously to load green indicator Alexa 488 (20 μM). Images were taken ~15–30 minutes after loading of the indicator. Alexa 488 and mCherry were excited by a femtosecond Ti:Sapphire laser (Chameleon Ultra; Coherent, Santa Clara, CA) at a wavelength of 880 nm.

Agonist application and magnetic stimulation

TRPV4 agonist, GSK1016790A (EMD Millipore, Billerica, MA), was puff applied with a brief (1 sec) air pressure by a glass pipette mounted on a Luigs-Neumann JUNIOR COMPACT manipulator (Luigs-Neumann GmbH, Ratingen, Germany) and positioned ~150 μm away from the recorded 293T cells. TRPV4-specific antagonist GSK205 (EMD Millipore), was bath applied. Magnetic stimuli were made using axially magnetized magnets, including a 3/8" cylinder magnet used in the previous study¹ and N42 1/16" × 1/4" block neodymium magnets purchased from K&J Magnetics. The magnetic intensity-distance relationships of these magnets were calculated with an HT20 Gauss Tesla meter (Shanghai Hengtong Cidian Technology Co., Ltd., Shanghai, China) (Fig S1). A Luigs-Neumann JUNIOR COMPACT manipulator was used to mount and rapidly position the magnets to 1.00 mm (for N42 block magnets) or 5.00 mm (for the 3/8" cylinder magnet) away from recorded cells to create a static magnetic field >50 mT. After stimulation, the magnets were rapidly withdrawn by 12–15 mm to eliminate magnetic stimuli. To determine the precise timing of applied magnetic field, we used an LED illuminator and a photodetector (Thorlabs Inc, Newton, NJ) to monitor the exact position of magnets mounted on a Luigs-Neumann JUNIOR COMPACT manipulator.

Statistical analysis

Statistical results were reported as mean±s.e.m. Animals or cells were randomly assigned into control or experimental groups and investigators were blinded to experiment treatments. No statistical methods were used to pre-determine sample sizes. Given the negative correlation between the variation and square root of sample number, n , the group sample size was typically set to be ~10–25 to optimize the efficiency and power of statistical tests (cf. see our previous publications^{4,5}). No animal or data point was excluded from the analysis. Statistical significances of the means ($p<0.05$; two sides) were determined using Wilcoxon non-parametric tests for paired samples. The data that support the findings of this study are available from the corresponding authors upon request.

Supplementary Material

Refer to Web version on PubMed Central for supplementary material.

ACKNOWLEDGEMENTS:

We are grateful to members of the Zhu laboratory for comments and technical assistance, many colleagues around the world for their support, encouragement, discussion, suggestions and/or sharing unpublished Magneto data. We appreciate Drs Chris Deppmann, Ali Güler and/or Manoj Patel for supplying TRPV4-P2A-ferritin-P2A-mCherry, Magneto-P2A-mCherry and Magneto-Ts-mCherry constructs and AAV DIO-Magneto and GFP-Cre viruses, and for the opportunity to visit and observe their electrophysiology experiments and multiple data cross-examination meetings in late 2015 after our many futile attempts to reproduce their findings. This study is supported in part by the Epilepsy Foundation postdoctoral fellowship No. 310443 (G.W.), Alzheimer's Association postdoctoral fellow-faculty transition Research Fellowship award AARF-19-619387 (P.Z.), NIH grants GM108989 (B.N.D.) and NS104670 (J.J.Z.). J.J.Z. is the Radboud Professor and Sir Yue-Kong Pao Chair Professor.

REFERENCES

1. Wheeler MA et al. Genetically targeted magnetic control of the nervous system. *Nature neuroscience* 19, 756–761, doi:10.1038/nn.4265 (2016). [PubMed: 26950006]
2. Meister M Physical limits to magnetogenetics. *eLife* 5, doi:10.7554/eLife.17210 (2016).
3. Nilius B & Szallasi A Transient receptor potential channels as drug targets: from the science of basic research to the art of medicine. *Pharmacological reviews* 66, 676–814, doi:10.1124/pr.113.008268 (2014). [PubMed: 24951385]
4. Wang G et al. $\text{Ca}_v3.2$ calcium channels control NMDA receptor-mediated transmission: a new mechanism for absence epilepsy. *Genes & development* 29, 1535–1551, doi:10.1101/gad.260869.115 (2015). [PubMed: 26220996]
5. Zhang L et al. Ras and Rap signal bidirectional synaptic plasticity via distinct subcellular microdomains. *Neuron* 98, 783–800, doi:10.1016/j.neuron.2018.03.049 (2018). [PubMed: 29706584]
6. Kole K et al. Assessing the utility of Magneto to control neuronal excitability in the somatosensory cortex. *Nature neuroscience*, submitted (2018).
7. Xu F-X et al. Magneto is ineffective in controlling electrical properties of cerebellar Purkinje cells. *Nature neuroscience*, submitted (2018).
8. Long X, Ye J, Zhao D & Zhang SJ Magnetogenetics: remote non-invasive magnetic activation of neuronal activity with a magnetoreceptor. *Science bulletin* 60, 2107–2119, doi:10.1007/s11434-015-0902-0 (2015). [PubMed: 26740890]
9. Stanley SA et al. Bidirectional electromagnetic control of the hypothalamus regulates feeding and metabolism. *Nature* 531, 647–650, doi:10.1038/nature17183 (2016). [PubMed: 27007848]
10. Wang G et al. An optogenetics- and imaging-assisted simultaneous multiple patch-clamp recordings system for decoding complex neural circuits. *Nature protocols* 10, 397–412 (2015). [PubMed: 25654757]

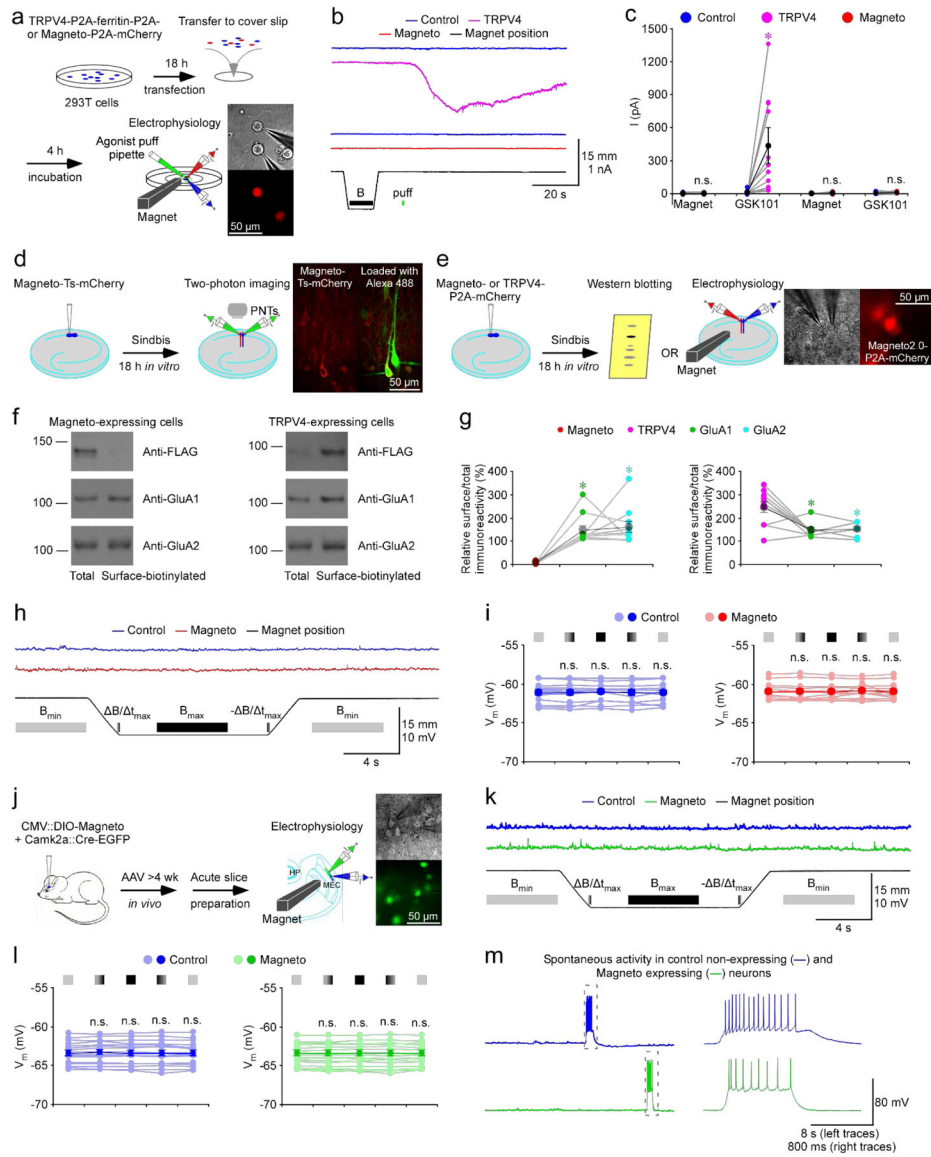


Figure 1. No magnetic effect in cells or neurons expressing Magneto2.0.

(a) Schematic drawing outlines the design of *in vitro* transfection, magnetic stimulation and electrophysiological recordings in TRPV4-P2A-ferritin-P2A-mCherry and Magneto-P2A-mCherry expressing cultured 293T cells. The right images show simultaneous whole-cell recordings from a pair of control non-expressing and Magneto-P2A-mCherry expressing cells under transmitted light (left) and fluorescence microscopy with RFP filter (right).

(b) Current recordings from neighboring control non-expressing and TRPV4-P2A-ferritin-P2A-mCherry expressing cells (left), and control non-expressing and Magneto-P2A-mCherry expressing cells (right) during magnetic stimulation and puff application of 100 nM TRPV4 agonist GSK1016790A (GSK101).

(c) Values of currents of control non-expressing and TRPV4-P2A-ferritin-P2A-mCherry expressing 293T cells during magnetic stimulation and puff application of GSK101 (Ctrl: -0.5 ± 0.9 pA; EXP: -1.8 ± 1.1 pA, $Z = -1.511$, $p = 0.12$ for control cells; Ctrl: 9.0 ± 5.3 pA;

EXP: 433.5 ± 132.6 pA, $Z=2.934$, $p<0.005$ for TRPV4 expressing cells; $n=11$). Values of currents of control non-expressing and Magneto-P2A-mCherry expressing 293T cells during magnetic stimulation and puff application of GSK101 (Ctrl: -0.2 ± 0.6 pA; EXP: 0.6 ± 1.4 pA, $Z=-0.175$, $p=0.86$ for control cells; Ctrl: 4.1 ± 2.2 pA; EXP: 7.1 ± 2.0 pA, $Z=1.293$, $p=0.20$ for Magneto expressing cells; $n=13$). Asterisk indicates $p<0.05$ (Wilcoxon tests).

(d) Schematic drawing outlines the design of *in vitro* Sindbis viral expression and two-photon imaging in cultured rat hippocampal slices. The right two-photon images show a pair of control non-expressing and Magneto-Ts-mCherry expressing CA1 pyramidal neurons after loading Alexa 488 with patch-clamp pipettes (left: mCherry channel only; right: mCherry and Alexa 488 red channels overlay; $n=5$ pairs from 2 animals).

(e) Schematic drawing outlines the design of *in vitro* Sindbis viral expression, biochemistry analysis, magnetic stimulation and electrophysiological recordings in cultured rat hippocampal slices. The right images show simultaneous whole-cell recordings from a pair of control non-expressing and Magneto-P2A-mCherry expressing CA1 pyramidal neurons under transmitted light (left) and fluorescence microscopy with RFP filter (right).

(f) Western blots of total and membrane surface-biotinylated recombinant Magneto2.0 and TRPV4 (both of which are FLAG tagged), and endogenous GluA1 and GluA2 in CA1 cells prepared from cultured rat hippocampal slices. Each lane loaded with 20 μ g proteins.

(g) Relative levels of membrane surface-biotinylated vs. total Magneto2.0 (Magneto2.0: $7.7 \pm 1.3\%$; GluA1: $148.0 \pm 17.8\%$, $n=11$, $Z=2.934$, $p<0.005$; GluA2: $160.2 \pm 23.3\%$; $n=11$, $Z=2.934$, $p<0.005$) and TRPV4 (TRPV4: $245.4 \pm 24.0\%$; GluA1: $145.5 \pm 9.4\%$, $n=10$, $Z=-2.396$, $p<0.05$; GluA2: $152.7 \pm 10.1\%$, $n=10$, $Z=-2.396$, $p<0.05$) compared to GluA1 and GluA2. Asterisks indicate $p<0.05$ (Wilcoxon tests).

(h) Recordings of membrane potentials of the pair of control non-expressing and Magneto-P2A-mCherry expressing CA1 pyramidal neurons before, during and after magnetic stimuli delivered with a K&J N42 1/16" permanent block magnet mounted on a micromanipulator.

(i) Values of membrane potentials of control non-expressing (Initial B_{\min} : -61.1 ± 0.3 mV; B/t_{\max} : -61.2 ± 0.4 mV, $Z=-1.038$, $p=0.28$; B_{\max} : -61.1 ± 0.3 mV, $Z=-0.105$, $p=0.92$; $-B/t_{\max}$: -61.2 ± 0.4 mV, $Z=-0.364$, $p=0.70$; Ending B_{\min} : -61.1 ± 0.3 mV, $Z=1.083$, $p=0.28$; Wilcoxon tests) and Magneto-P2A-mCherry (Initial B_{\min} : -60.9 ± 0.3 mV; B/t_{\max} : -61.0 ± 0.3 mV, $Z=-0.664$, $p=0.51$; B_{\max} : -61.0 ± 0.3 mV, $Z=-1.103$, $p=0.31$; $-B/t_{\max}$: -60.8 ± 0.3 mV, $Z=-0.314$, $p=0.75$; Ending B_{\min} : -61.0 ± 0.3 mV, $Z=-0.734$, $p=0.46$; Wilcoxon tests) expressing CA1 pyramidal neurons when the permanent magnet was away from (light), approaching to (light-dark transient color), close to (dark), retracting from (dark-light transient color), and away from (light) recorded neurons ($n=13$ from 6 animals). Note no difference in membrane potential in control non-expressing and Magneto-P2A-mCherry expressing CA1 pyramidal neurons in all the experimental stages ($p>0.05$; Wilcoxon tests).

(j) Schematic drawing outlines the design of *in vivo* AAV viral expression of CMV::DIO-Magneto and Camk2a::Cre-EGFP, *ex vivo* magnetic stimulation and electrophysiological recordings in acutely prepared mouse MEC slices. The right images show simultaneous whole-cell recordings from a pair of control non-expressing and DIO-Magneto/Cre-GFP expressing MEC L2/3 pyramidal neurons under transmitted light (left) and fluorescence microscopy with GFP middle filter (right).

(k) Recordings of membrane potentials of the pair of control non-expressing and DIO-Magneto/Cre-GFP expressing MEC L2/3 neurons before, during and after magnetic stimuli delivered with a K&J N42 1/16" permanent block magnet mounted on a micromanipulator.

(l) Values of membrane potentials of control non-expressing (Initial B_{\min} : -63.4 ± 0.3 mV; B/ t_{\max} : -63.4 ± 0.4 mV, $Z=1.018$, $p=0.31$; B_{\max} : -63.4 ± 0.4 mV, $Z=0.213$, $p=0.83$; - B/ t_{\max} : -63.4 ± 0.4 mV, $Z=0.734$, $p=0.46$; Ending B_{\min} : -63.4 ± 0.3 mV, $Z=-1.065$, $p=0.29$) and Cre-GFP/DIO-Magneto2.0 (Initial B_{\min} : -63.4 ± 0.3 mV; B/ t_{\max} : -63.4 ± 0.4 mV, $Z=-0.024$, $p=0.98$; B_{\max} : -63.4 ± 0.4 mV, $Z=0.166$, $p=0.87$; - B/ t_{\max} : -63.4 ± 0.4 mV, $Z=0.166$, $p=0.87$; Ending B_{\min} : -63.4 ± 0.3 mV, $Z=-1.207$, $p=0.23$) expressing MEC L2/3 pyramidal and stellate neurons when the permanent magnet was away from (light), approaching to (light-dark transient color), close to (dark), retracting from (dark-light transient color), and away from (light) recorded neurons ($n=17$ from 11 animals). Note no difference in membrane potential in control non-expressing and DIO-Magneto/Cre-GFP expressing MEC L2/3 neurons in all the experimental stages ($p>0.05$; Wilcoxon tests).

(m) Recordings of spontaneous events in the pair of control non-expressing and DIO-Magneto/Cre-GFP expressing MEC L2/3 neurons. Note that the spontaneous suprathreshold events in the gray dash line boxes are shown again in an expanded time scale in the right.